This paper appears in IEEE Transactions on Control Systems Technology.
https://doi.org/10.1109/TCST.2016.2594584

A Passivity-based approach for Stable Patient-Robot Interaction in Haptics-enabled Rehabilitation Systems: Modulated Time-domain Passivity Control (M-TDPC)*

S. Farokh Atashzar, *Student Member, IEEE*, Mahya Shahbazi, *Student Member, IEEE*, Mahdi Tavakoli, *Member, IEEE*, Rajni V. Patel, *Life Fellow, IEEE*

***Abstract*—In this paper, a novel passivity-based technique is proposed to (a) analyze and (b) guarantee the stability of haptics-enabled robotic/telerobotic systems when there is a possibility of having a source of nonpassivity (namely, a nonpassive environment) in addition to the conventional nonpassive component in teleoperation systems (namely, a delayed communication channel). The need for the proposed technique is motivated by safe and optimal implementation of haptics-enabled robotic, cloud-based and remote rehabilitation systems. The objective of the controller proposed in this paper is to perform minimum alteration to the system transparency, in a dynamic and patient-specific manner, by utilizing quantifiable biomechanical capability of the user's limb (i.e. Excess of Passivity) in dissipating interactive energies to guaranteeing human-robot interaction safety, in the context of the Strong Passivity Theorem (SPT). The proposed controller is named Modulated Time-Domain Passivity Control (M-TDPC) approach and is a new member of the family of state-of-the-art TDPC techniques. Simulations and experimental results are presented in support of the proposed technique and the developed theory.**

List of Acronyms

TDPC: Time-Domain Passivity Control, **PTDPC:** Power-domain TDPC, **M-TDPC:** Modulated TDPC, **EOP:** Excess of Passivity, **SOP:** Shortage of Passivity, **LOP:** Lack of Passivity, **NP:** Neural Plasticity, **RT:** Resistive Therapy, **AT:** Assistive Therapy, **VR:** Virtual Reality, **DOF:** Degrees of Freedom, **HRR:** Haptics-enabled Robotic Rehabilitation, **HTR:** Haptics-enabled Telerobotic Rehabilitation, **PVT:** Programmable Virtual Therapist, **PAT:** Power Assistive Therapy, **CAT:** Coordination Assistive Therapy, **VE:** Virtual Environment, **WPT:** Weak Passivity Theorem , **SPT:** Strong Passivity Theorem, **ISP:** Input Strictly Passive, **OSP:** Output Strictly Passive , **INP:** Input NonPassive, **ONP:** Output NonPassive, **PD:** Passivity Differential.

* This research was supported by the Canadian Institutes of Health Research (CIHR) and the Natural Sciences and Engineering Research Council (NSERC) of Canada under the Collaborative Health Research Projects (CHRP) Grant #316170; an NSERC Collaborative Research and Development Grant # CRDPJ 411603-10 with industrial partner, Quanser Inc.; the AGE-WELL Network of Centres of Excellence under the project AW CRP 2015-WP5.3; the Canada Foundation for Innovation (CFI) under grant LOF 28241; and the Alberta Innovation and Advanced Education Ministry under Small Equipment Grant RCP-12-021. S.F. Atashzar, M. Shahbazi, and R.V. Patel are with Canadian Surgical Technologies and Advanced Robotics (CSTAR), and with the Dept. of Electrical and Computer Engineering, Western University, Canada (email: satashza@uwo.ca, mshahba2@uwo.ca, rvpatel@uwo.ca). R.V. Patel is also with the Dept. of Surgery at Western University. M. Tavakoli is with the Department of Electrical and Computer Engineering, University of Alberta, Canada (email: mahdi.tavakoli@ualberta.ca). The initial concept of this work was partially presented in the conference paper [1].

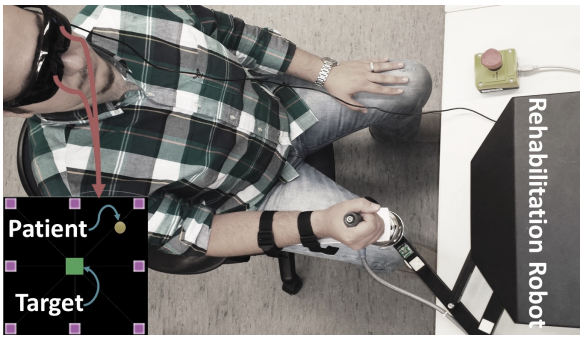

Fig. 1. The HRR system and the VR environment used in this paper.

I. Introduction and Preliminaries

Based on the World Health Organization statistics and according to epidemiology studies, there are more than 15 million people who experience stroke each year [2], [3]. In addition, official numbers show that the population of senior adults are rapidly increasing and is expected to be more than double by 2050 compared to the numbers in 2013 [4]. This fact is called society ageing, which directly increases the incidence of age-related conditions including post-stroke motor disabilities. The affected population require labour-intensive motor therapy services for extended periods which places a significant burden on therapists and healthcare systems. In many cases, the only offered service is limited and often delayed outpatient therapy. The situation is worse for patients in remote areas with limited access to sophisticated rehabilitation clinics [5]. One solution is to develop cloud-based technologies that provide efficient, optimal and affordable means of in-hospital and in-home rehabilitation to help patients regain their lost motor functions through utilizing Neural Plasticity (NP). NP is brain remodeling that happens in chemical (synaptic) and structural (non-synaptic) levels and can result in regaining lost motor functions and enhancement of standard sensorimotor performance metrics in post-stroke patients [6], [7]. In this context, Haptics-enabled Robotic Rehabilitation (HRR) has been demonstrated to accelerate NP and neural recovery [8], [9], [10].

There are two types of therapeutic procedures that can be delivered using HRR systems: (a) Assistive Therapy (AT), mostly administered in early stages of rehabilitation, and (b) Resistive Therapy (RT), mostly considered for later stages of therapy. During the AT, the haptic robot helps patients to

perform task-based movements that need high power/force, large motion range and good targeting accuracy. AT is mostly applied in order to trigger and accelerate NP. During RT, the haptic robot resists the movements initiated by the patient [8], [10] with the goal of helping patients to develop and equalize musculoskeletal strength.

Conventional HRR systems are composed of three major components: (a) a powerful haptic robot that registers the patient's impaired limb force/motion profiles and applies the assistive/resistive forces; (b) a game-like virtual reality (VR) software environment that provides visual cues and demonstrates the desired path of motion; and (c) a Programmable Virtual Therapist (PVT) algorithm that uses the measured patient's force/motion data and determines the needed AT/RT to be delivered to the patient's impaired limb [8], [10], [11]. A representative HRR system used in this paper is shown in Fig. 1.

Research has shown that key to an effective therapy is to modify the type, duration and intensity of exercises, considering the state and progress of the patient's motor recovery [12]. There are some adaptive techniques proposed in the literature to tune the parameters of the PVT [13], [14] based on some sensorimotor measurements. However, direct, intuitive and interactive contribution of a human therapist is bypassed using PVT-based HRR systems. This limits the ability of the human therapist in choosing the best position/force therapeutic trajectories and tasks for patient rehabilitation and motor assessment.

In order to deal with this issue, the authors have recently proposed and simulated a bilateral Haptics-enabled Telerobotic Rehabilitation (HTR) architecture [15], [16] that can fuse the advantages of conventional HRR systems and the skills of a human therapist in the loop and provide patients with an "augmented" therapeutic environment instead of virtual therapy. The concept is close to comparing the augmented reality over virtual reality, thus we proposed to call HTR an augmented therapy framework. A schematic of the implemented HTR system, including the proposed stabilizer (which will be explain later), is given in Fig. 2. By virtue of telerobotics-aided telepresence, HTR also enables remote/in-home assessment and therapy delivery for post-stroke patients. This directly responds to a need of patients in areas far from sophisticated rehabilitation centres and is helpful given the current trend in modern healthcare systems to embrace the possibilities offered by "telemedicine" (providing medical services and stroke cares over distance to enhance accessibility) [5],[17], [18].

Besides clear advantages to the use of HRR and HTR technologies for in-clinic and in-home assessment and rehabilitation, the safety of human-robot interactions (and specifically patient-robot interaction) could be a major concern [19], which should be considered, studied and guaranteed in an appropriate manner, while maximizing the system transparency and effectiveness. Realizing the aforementioned need is more challenging when high control efforts are needed for a patient during rehabilitation to deliver a prescribed therapy (especially when the system is used for in-home usages). To make it more clear, consider

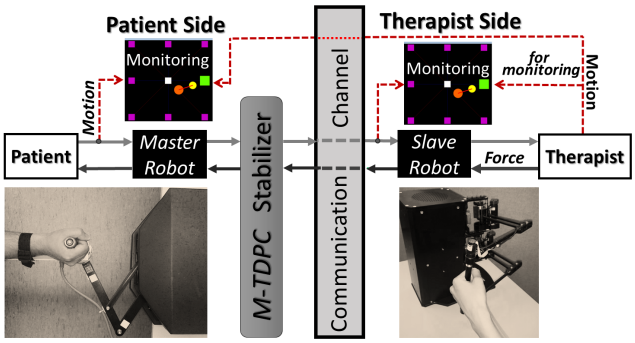

Fig. 2. A schematic of the implemented HTR system used in this paper. The virtual environment is shared between the therapist and the patient where the orange and yellow circles correspond to the patient's and therapist movements, respectively.

a patient who has unbalanced high tone of muscular system (this condition is a common side effect of stroke). In order to assist this patient in executing rehabilitation exercises (such as workspace stretching during object tracking), it is needed to apply high forces compare to a patient who does not have this symptom. In this case, the behavior of the rehabilitative system should be different for these two patients while the stability must be guaranteed for both. Also, as shown in the rest of this paper, assistive forces generated by a remote human or a cloud-based software result in a nonpassive interconnection which can potentially challenge the stability. Consequently, proper stability analysis and development of new stabilization techniques which perform minimal transparency modification is a practical need. In this paper, the mentioned concern is studied for haptics-enabled systems (specifically for HRR and HTR architectures). We study and guarantee patient-robot interaction safety using a novel passivity-based technique entitled Modulated Time Domain Passivity Control (M-TDPC), which can optimize the delivered transparency by utilizing the passivity characteristics of the user's hand biomechanics, while guaranteeing stability. For this purpose first a new stability condition is developed, in the context of SPT. Then, the proposed M-TDPC approach is defined. The stability condition shows that under specific quantifiable conditions, it is possible to avoid applying damping into the interconnection, during the operation, while still guarantee the system stability regardless of nonpassivity of the communication and/or the environment.

The rest of this paper is organized as follows. In Section II, the motivation and an overview of the proposed M-TDPC technique are given. In Section III, the mathematical modeling and transparency analysis are presented. In Section IV, the therapy passivity is analyzed. In Section V the proposed stability analysis for assistive and resistive therapies is introduced. In Section VI, the M-TDPC stabilizing scheme is explained. Simulations results are given in Section VII and the experimental evaluations are presented in Section VIII. Finally, the paper is concluded in Section IX.

II. Motivation and Overview of M-TDPC Scheme

The propose M-TDPC technique answers how one can minimally adjust the intensity of the potentially nonpassive therapeutic interventions prescribed by the virtual/human therapist in an HRR/HTR system (in the context of SPT) to ensure patient safety and human-robot interaction stability. The proposed controller is a new member of the family of state-of-the-art TDPC controllers [20],[21],[22]. In this paper, we will show how to utilize biomechanical characteristics of the user's hand, in the context of SPT [23], to deliver patient-specific customized therapeutic forces that can guarantee the system stability and causes minimal disruptions to transparency.

Note that some of the stabilizers developed in the literature such as the wave variable approach are composed of two transformations: one before the communication channel and one after. If the delay in the system converges to zero, the two transformations cancel each other out to keep the transparency ideal. However, in this paper, we need the controller to be functional even if the delay is zero since there is a second source of nonpassivity in the system under study (which can be due to assistive could-based virtual software or a human therapist in the loop or a combination of the two). This has been realized by the proposed M-TDPC approach, which can deal with both delay-induced and environment-induced nonpassivities separately and simultaneously.

The proposed M-TDPC approach is also motivated by ensuring human-robot interaction stability without imposing the pre-fixed conservative saturating force caps (such as those in [9], [24]). Using M-TDPC the haptic rehabilitation robot will be able to apply maximum forces considering the specific biomechanical capabilities of the patient's limb in absorbing therapeutic energies. This promises to result in therapeutic interventions much closer to those prescribed.

The design framework is based on the core hypothesis that *"when there is nonpassivity in haptics-enabled rehabilitation systems (HRR and HTR) caused by (a) the nonpassive behavior of a virtual/human therapist and/or (b) the delayed communication network, the closed-loop haptics-enabled system remains passive and stable if the quantifiable Excess of Passivity (EOP) of the nonlinear biomechanical impedance of the patient's limb can compensate for the total Shortage of Passivity (SOP) caused by the aforementioned nonpassivities"*. The hypothesis is validated in this paper in the context of SPT.

This principle is then used to design the M-TDPC strategy that (a) identifies the EOP of the patient's limb prior to the therapeutic task execution, (b) monitors the extent of nonpassivity of the administered therapy delivered through the communication network during the operation, (c) calculates in real-time the "minimum necessary" energy, to be damped by the proposed controller, and (d) injects a time-varying damping factor to compensate for the energy. The controller keeps the injected damping as small as possible, using the identified patient's limb EOP, causes minimal alterations to the prescribed therapy and allows the nonpassive energy (i.e., therapeutic assistance) to optimally flow from the (virtual or actual) therapist to the patient.

The M-TDPC technique can not only be used for (a) HRR and HTR systems (to relax the limitation on the therapy intensity and passivity and deal with potential delays), but can also be used for (b) conventional haptic interactions (to deal with the delay-induced instabilities and enhance the system transparency).

III. System Modeling and Transparency Analysis

In order to model human-robot interaction to analyze the stability and implement appropriate stabilizing controller for high-intensity therapy, transparent two-channel bilateral model [25] is considered which is an extension of Lawrence's four-channel architecture [26]. For both the HTR and HRR architectures, the patient is at the master robot to allow him/her to apply different motion trajectories. Also, for the HTR architecture, the human therapist is at the slave robot so that he/she can feel the patient's motions and provide resistive/assistive forces in response in order to administer the desired therapy. For the case of HRR architecture, software-based therapy is provided by a virtual environment that generates therapeutic forces in response to the measured patient's movements. The virtual-reality environment provides visual cues for the patient using a head-mounted display or a table-top screen.

A. Local Interaction Modeling

In this subsection, the models considered regarding (a) patient-robot interaction for both HTR and HRR architectures, (b) therapist-robot interaction for HTR architecture, and (c) virtual therapist for HRR architecture are presented.

- ***Patient-robot Interaction***

A local feedback linearization algorithm [27] is considered for the master robot to compensate for nonlinear dynamics of the robot. As a result, the linearized model for the Patient-Robot (P-R) interaction are

$$z_m(t) * v_p(t) = u_{cm}(t) + f_p(t) \tag{1}$$

In (1), t is time, $*$ is the convolution operator, $z_m(t)$ is the impulse response of the linearized master robot dynamics, $u_{cm}(t)$ is the control input for the master robot delivering needed therapy, $v_p(t)$ is the patient's hand velocity, and $f_p(t)$ is the force applied by the patient to the master robot. The patient's force can be decomposed into "voluntary", i.e. $f_p^*(t)$, and "reactive", i.e. $f_{react}(t)$, components as

$$f_p(t) = f_p^*(t) - f_{react}(t), \quad \text{where} \quad f_{react} = z_p(v_p, t) \tag{2}$$

In (2), $z_p(v_p,t)$ is the non-autonomous nonlinear impedance model considered for the mechanical reaction of the patient's limb in response to the master robot movements. This relaxes the conventional assumption on linearity of the operator's hand, which is not the case in practical situations. Also, $f_p^*(t)$ is the voluntary component of force applied by the musculoskeletal system of the patient's hand to generate

motion and perform tasks. The other possible representation of the aforementioned patient's force decomposition is admittance notation, given in

$$v_p = \Omega_p(f_p^*(t) - f_p(t), t) \tag{3}$$

- ***Therapist-Robot Interaction***

This part focuses on the dynamical behavior of the in-the-loop human therapist for the HTR architecture. A general model is considered for the therapist's behavior to cover a wide range of nonlinear, non-autonomous and nonpassive dynamical effects of the therapists, in realistic cases. Placing the human therapist at the slave side of the telerehabilitation system allows him/her to intuitively assist/resist patient's trajectories based on his/her therapeutic skills. Same as the master side, a local feedback linearization algorithm is considered for the slave robot to compensate for the robot nonlinearities. The Therapist-Robot (T-R) interaction model is

$$z_s(t) * v_{th}(t) = u_{cs}(t) + f_{th}(t), \tag{4}$$

where $z_s(t)$ is the impulse response of the linearized slave robot's dynamics, $u_{cs}(t)$ is the control input for the slave robot, $v_{th}(t)$ is the therapist's hand velocity, and $f_{th}(t)$ is the force, applied by the therapist to the slave robot in order to administer therapy. The therapist's force model is

$$f_{th}(t) = z_{th}(v_{th}(t), f_{th}^*(t), t) \tag{5}$$

In (5), z_{th} is the nonlinear non-autonomous reaction provided by the therapist to deliver a therapeutic response. In this paper, z_{th} is called "therapeutic reaction dynamics" and is function of the delivered movement to the therapist by the slave robot v_{th}, the exogenous force of the therapist f_{th}^*, and time. f_{th}^* can be considered as an additive term. During a therapy session, the therapist tunes her/his reaction z_{th} to generate a desirable therapeutic response based on the patient's need. This behavior can result in either dissipating the energy provided for the therapist (when the therapist is performing a resistive therapy), or elevating the provided energy to perform faster/larger movements (when the therapist is performing an assistive therapy). That is why resistive therapy is passive in contrast to assistive therapy (more discussions are given later in this paper).

- ***Considered Modeling Assumptions***

As a result of the defined interaction models, the following assumptions are considered to analyze the stability of the system and design stabilizer for realistic conditions:

1) The therapist is allowed to behave as a nonpassive dynamical terminal for the interconnection. This enables him/her to inject energy into the interaction as is needed in assistive therapy.
2) The therapist can behave as a nonlinear non-autonomous system. This enables him/her to administer various types of therapy, tune the therapy intensity, and switch between different therapeutic regimes.
3) The reaction component of the patient's hand $z_p(v_{th}, t)$ is considered to be a passive nonlinear non-autonomous mechanical system. Special case for $z_p(v_{th}, t)$ is the common passive mass-spring-damper model widely used in the literature to model the dynamical reaction of human upper-limb [28], [29], [30]. In this work no restriction is considered for linearity of $z_p(v_{th}, t)$ to analyze/guarantee the stability in a more realistic condition.
4) The communication network can be subject to time-varying delays (which is the conventional source of nonpassivity in haptics-enabled systems).

- ***The Case of Virtual Therapist***

The virtual therapist model is in fact a subcategory of the above-given therapist-robot interaction dynamics where there is no slave robot. Instead of having a general nonlinear model for a human therapist z_{th} we have a multiplicative linear model (defined below) that generates therapeutic forces. Similar to the behavior of a human therapist, there are two major types of virtual therapy that can be programmed, namely, resistive and assistive therapies. For resistive virtual therapy in HRR systems, the therapist's side model is

$$f_{th}(t) = D_{th}(t) \cdot v_{th}(t) \text{ where } v_{th}(t) = \hat{v}_p(t),\ D_{th}(t) < 0 \tag{6}$$

In (6), $f_{th}(t)$ is the therapeutic force generated by the programmed virtual therapist in response to the measured patient's hand movement $\hat{v}_p(t)$; $D_{th}(t)$ is the therapeutic intensity gain which is negative for the case of Resistive Therapy (RT), when the patient feels a viscous interaction resisting against her/his movement.

For the case of assistance, two different behaviors can be programmed, namely, Power Assistive Therapy (PAT) and Coordination Assistive Therapy (CAT). For PAT, we have

$$f_{th}(t) = D_{th}(t) \cdot v_{th}(t) \text{ where } v_{th}(t) = \hat{v}_p(t),\ D_{th}(t) > 0 \tag{7}$$

Positive values for $D_{th}(t)$ lets the patient feel amplified power while providing movements and performing tasks. Using PAT, the system provides assistive forces in the same direction as that of the patient's movements. As a result, the patient with reduced muscular power can perform tasks require higher power, larger workspace, and faster motions.

For the second type of assistance (CAT), the goal is to coordinate the patient's movements towards the desirable path of therapy. This is useful when patients have coordination deficits due to stroke. CAT provides patients with a correct model of sensorimotor fusion during task performance. The therapist-side interaction model for CAT is

$$\begin{gathered} f_{th}(t) = D_{th}(t) \cdot e_{th}(t), \quad D_{th} \geq 0 \\ \text{where: } e_{th}(t) = x_{goal}^*(t) - x_{th}(t), \\ x_{th}(t) = \int_0^t v_{th}(\tau)\, d\tau, \\ \text{and} \quad v_{th}(t) = \hat{v}_p(t). \end{gathered} \tag{8}$$

In (8), x_{goal}^* is the varying target position displayed to the patient, and the therapeutic intensity gain D_{th} is a corrective factor that makes the patient movement follow the target.

B. Transparency Analysis

In order to provide the patient with high-fidelity administered therapy and the therapist (for the case of HTR)

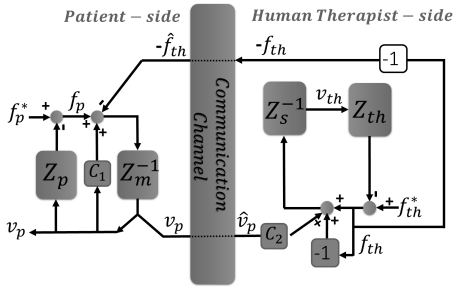

Fig. 3. The utilized transparent Two-channel HTR architectures.

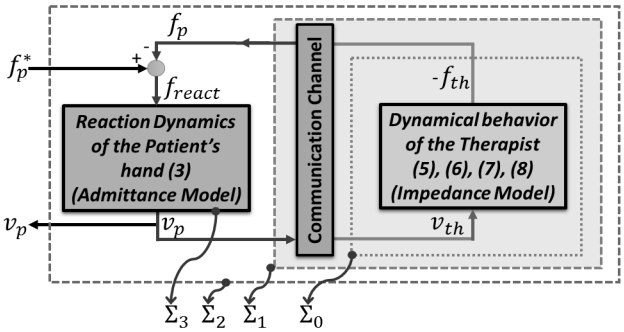

Fig. 4. The overall schematic of the resulting interconnection. The subsystem Σ_1 is called the "therapy terminal" which consists of the communication and any behavior of the therapist. Also, Σ_2 is the entire interaction which gets f_p^* as the input and provides v_p as the output. Σ_3 is the admittance model of the patient's limb mechanical reaction

with an accurate feel of the patient's limb movement trajectories, a two-channel transparent teleoperation architecture, proposed by the authors in [25], is considered. The utilized architecture is a modification of the Lawrence's four-channel scheme [26], which uses the minimum number of communication channels (two) while guaranteeing the system's transparency. To implement the aforementioned architecture, the control signals $u_{cm}(t)$ is designed at the master side (for both HTR and HRR systems) as

$$u_{cm}(t) = c_1(t) * v_p(t) + \hat{f}_{th}(t) \quad where \quad c_1(t) = z_m(t). \quad (9)$$

Also, the control signal $u_{cs}(t)$ is implemented at the slave side for the case of HTR system as

$$u_{cs}(t) = -f_{th}(t) + c_2(t) * \hat{v}_p(t) \quad where \quad c_2(t) = z_s(t). \quad (10)$$

In (9) and (10), $\hat{f}_{th}(s)$ is the delayed received therapeutic force at the patient-side, sent through the first (slave to master) communication channel, and $\hat{v}_p(t)$ is the received patient's hand velocity at the therapist-side, sent through the second (master to slave) communication channel. In order to enable the case of remote rehabilitation, the communication is considered subjected to time-varying delays defined by $\tau_1(t)$ for the first channel and by $\tau_2(t)$ for the second channel. Consequently, we have $\hat{f}_{th}(t) = f_{th}(t - \tau_1(t))$, and $\hat{v}_p(t) = v_p(t - \tau_2(t))$. The schematic of the designed transparent two-channel haptics-enabled architecture for the case of HTR is given in Fig. 3.

It should be noted that for conventional HRR systems, $\tau_1(t)$ and $\tau_2(t)$ might be zero. However, considering the recent tendency in the literature for implementing internet-based cloud rehabilitation systems [31] and to keep the generality of the technique, in this paper, we have considered $\tau_1(t)$ and $\tau_2(t)$ to have non-zero values for both HRR and HTR systems. Combining the control signals defined in (9) and (10) with the dynamics of the master and slave robots given in (1) and (4), for the HTR architecture, the force-feedback transparency and velocity tracking of the teleoperation system can be shown as

$$f_p(t) = -\hat{f}_{th}(t), \quad (11)$$

$$v_{th}(t) = \hat{v}_p(t). \quad (12)$$

For HRR systems, force-feedback transparency (11) can be achieved through similar calculations based on the defined $u_{cm}(t)$ given in (9). In addition, velocity tracking (12) is set through software for HRR systems as there is no slave robot at the therapist's side.

Consequently, the resulting dynamics for both HTR and HRR systems is a two-channel interconnection (shown in Fig. 4) between the admittance model of the patient's dynamics Σ_3 and impedance model of the therapist's reaction dynamics Σ_0, communication through the network. Note that the admittance Σ_3 has force as input and motion as output and is defined by (3) as Ω_p. Also, the impedance model Σ_0 has motion as input and force as output, and is defined by (5) for HTR, by (6) for HRR-RT, by (7) for HRR-PAT, and by (8) for HRR-CAT. As shown in Fig. 4, the sources of potential nonpassivity (therapist's behavior and communication delays) can be bundled as the therapy terminal Σ_1. This enables us to analyze the HTR and HRR interconnections from the perspective of input-output energy exchange between Σ_1 and Σ_3. As a result, in the rest of this paper, we will focus on the inclusive interconnection shown in Fig. 4 and will developed the stability condition and stabilizing scheme for this interconnection. Consequently, studying the interconnection shown in Fig. 4 accounts for any behavior of the therapist, including assistance, resistance, coordination and mixed therapy together with different possibilities of therapists including virtual therapist and human therapist, plus communication delays.

IV. Passivity Evaluation for Assistive and Resistive Therapies

In order to resist a patient's movements, the therapist needs to dissipate the energy provided by the patient. This results in giving the patient feel of moving in a viscous environment. Also, in order to assist movements of a disabled patient, the therapist needs to elevate the energy by injecting it into the interconnection to allow for having faster movements, higher workspaces and more accurate task executions.

Intuitively speaking, it can be said that energy dissipation during resistive therapy is passive, while energy elevation resulting from assistive therapy is nonpassive. To show this concept, in this section, we mathematically evaluate PAT,

CAT and RT cases using the developed models for HRR presented in the previous section. The goal is to show differences between the nature of resistance and that of assistance by analyzing their energy characteristics. The main statement of this section is: *resistive therapy is passive by it's nature and assistive therapy is either nonpassive or potentially-nonpassive*.

To show this, first, the mathematical definition of a passive system with input vector $u_{in}(t)$, output vector $y_{out}(t)$, and initial energy β at $t=0$ is [23]:

Definition I. *If there is a constant β such that for all $t \geq 0$ we have*

$$\int_0^t u_{in}(\tau)^T \cdot y_{out}(\tau)\, d\tau \geq \beta, \tag{13}$$

the system is passive. •

First, consider the therapy terminal Σ_1 in Fig. 4. To focus on studying the passivity of therapies, the communication time delays ($\tau_1(t)$ and $\tau_2(t)$) are considered zero. Also, we assume that the system starts from a rest condition, so the initial energy β is considered to be zero. Note that for Σ_1, we have $u_{in} = v_p$ and $y_{out} = f_p$. Consequently, considering (11), (12), and (13), the passivity of Σ_1 can be evaluated by determining the sign of

$$\int_0^t -f_{th}(\tau)^T \cdot v_{th}(\tau)\, d\tau. \tag{14}$$

Combining (14) and model (6), defined for PAT and RT, we have:

$$\begin{aligned} &\int_0^t -f_{th}(\tau)^T \cdot v_{th}(\tau)\, d\tau = \\ &\int_0^t -v_{th}(\tau)^T \cdot D_{th}(\tau)^T \cdot v_{th}(\tau)\, d\tau. \end{aligned} \tag{15}$$

Considering (15) and assigning negative definite diagonal D_{th} for resistive behaviors results in positive sign for the integral in (14). This means that, the resistive behavior of a therapist dissipates energy of the system and it is passive (considering the definition of passive systems (13)). Similar calculations can be performed for PAT where we have positive definite D_{th}. This results in having negative value for the integral in (14), which means that PAT injects energy into the system and is nonpassive.

For the case of CAT, we have

$$\begin{aligned} &\int_0^t -f_{th}(\tau)^T \cdot v_{th}(\tau)\, d\tau = \\ &\int_0^t -e_{th}(\tau)^T \cdot D_{th}(\tau)^T \cdot v_{th}(\tau)\, d\tau. \end{aligned} \tag{16}$$

In this case, the sign of the passivity integral can not be defined and is directly related to the sign of tracking error e_{th} (which can be positive or negative in each time stamp) and the history of it. As a result, it is not possible to assign a definite sign for the passivity integral which means that the system can inject energy into the interconnection and challenge the stability of the system. Consequently, CAT is potentially nonpassive.

In summary, the natures of increasing the power during task performance or coordinating the patient during rehabilitation can render therapy terminal Σ_1 nonpassive and challenge the stability of the system, even if the communication delay is zero. In contrast, resistive therapy dissipates the interconnection energy as a passive component.

It should be noted that in the presence of the communication delays, there will be two sources of nonpassivity in the system. As mentioned earlier, in this paper both possible sources of nonpassivity are bundled into the one-port therapy terminal Σ_1. In Section V, a new framework will be proposed that allows for evaluating the stability condition of the system even if Σ_1 is nonpassive. Then in Section VI, the framework will be used to develop the proposed stabilizing scheme (M-TDPC).

It should be highlighted that since the analysis and stabilizing schemes proposed in this paper account for any nonpassive behavior of Σ_1, not only they can be used for nonpassive rehabilitation systems, but also they can be used for conventional time-delayed telerobotic architectures and haptics systems to handle delay-induced instability.

V. Proposed Stability Analysis Framework Using EOP/SOP Definitions

Considering Fig. 4, in order to analyze the stability of the system and calculate the stability condition of the interconnection in the presence of nonpassive Σ_1, the following hypothesis is proposed and mathematically proven in this section:

Hypothesis I. *When there is a nonpassive therapy terminal (Σ_1) in a haptics-enabled rehabilitation system due to (a) nonpassive behavior of a therapist and/or (b) nonpassive communication network, the closed-loop system can still remain stable if the excess of passivity of the patient's limb mechanical dynamics can compensate for the shortage of passivity of the therapy terminal Σ_1.* •

The remainder of this section focuses on how this hypothesis can be mathematically proven. It should be noted that, there is an important difference between the conventional use of passivity theory and the way used in this paper based on SPT, as discussed below.

Remark 1. In the conventional use of passivity theory [23], [32], assuming passive operator and environment terminations for a haptics-enabled system, ensuring the communication passivity provides an interconnection of cascaded passive subsystems, which remains stable. This is called the Weak Passivity Theorem (WPT), which is widely used in the literature of conventional telerobotic systems [22] to analyze and guarantee system stability [33]. The communication delay is considered to be the sole source of nonpassivity in this regard. However, for the case of assistive HTR and HRR systems, even if the communication channel is ideally passive, the passivity of the resulting cascaded interconnection Σ_2 is not guaranteed because Σ_1 is still nonpassive. •

Remark 2. Contrary to conventional haptics-enabled teleoperation systems, the nonpassive behavior caused by assistive therapy is exactly what is needed for therapeutic

application, should not be interpreted as an unwanted, and should not be cancelled out by the control system. It is counterproductive to separately passify the nonpassive therapist since it defeats the very purpose of power assistance and coordination by damping all the needed therapeutic energy. Consequently, to preserve the patient-robot interconnection safety while still allowing the nonpassive therapy terminal Σ_1 to inject energy, the passivity of the *entire* interconnection Σ_2 should be analyzed (instead of passivity of isolated components considered in WPT-based approaches). This has correlations with the definition of the SPT given in [23], [34] and utilized in this paper to analyze and guarantee the entire system's passivity. •

For this goal and to validate Hypothesis I, first the mathematical definitions of input-passive modeling, output-passive modeling, EOP and SOP for a system with input vector $u_{in}(t)$, output vector $y_{out}(t)$, and initial energy β at $t=0$ are taken from [23], [35], [36], as given below. Note that the system is considered to be square which means that the number of inputs and outputs are equal.

Definition II. *If there is a constant β such that for all $t \geq 0$ we have*

$$\int_0^t u_{in}(\tau)^T \cdot y_{out}(\tau)\, d\tau \geq \beta + \delta \cdot \int_0^t u_{in}(\tau)^T \cdot u_{in}(\tau)\, d\tau, \quad (17)$$

for $\delta \geq 0$, the system is Input Strictly Passive (ISP) with an excess of passivity (EOP) equal to δ. Also, if we have $\delta < 0$, the system is Input Nonpassive (INP) with the Shortage of Passivity (SOP) of δ. •

Definition III. *If there is a constant β such that for all $t \geq 0$ we have*

$$\int_0^t u_{in}(\tau)^T \cdot y_{out}(\tau)\, d\tau \geq \beta + \xi \cdot \int_0^t y_{out}(\tau)^T \cdot y_{out}(\tau)\, d\tau, \quad (18)$$

for $\xi \geq 0$, the system is Output Strictly Passive (OSP) and the EOP is ξ. Also if we have $\xi < 0$, the system is Output Nonpassive (ONP) and the SOP is ξ. •

Remark 3. It has been shown that passive systems (including ISP and OSP) are asymptotically stable. In addition, an OSP systems is also L_2 stable with finite L_2 gain less than or equal to $1/\xi$, where ξ is the EOP of the OSP model [27]. The mathematical description of L_2 stability for an OSP system is given below (where $\alpha_0 \geq 0$ is related to the initial energy and is zero in this paper since the system is assumed to start from rest):

$$\|y_o(t)\|_{L_2} \leq 1/\xi \cdot \|u_i(t)\|_{L_2} + \alpha_0. \quad (19)$$

Considering (19), ξ defines an upper-bound on the energy of the system's output, based on the input energy. •

In order to validate Hypothesis I, consider the entire system as the one-port network Σ_2 shown in Fig. 4. Σ_2 consists of a nonpassive therapy-terminal impedance Σ_1 and a passive patient's reaction admittance Σ_3. The exogenous force $f_p^*(t)$ is the input for Σ_2 and the velocity of the patient's hand $v_p(t)$ is the response to this input. Consequently, considering (13), to first guarantee the passivity of the entire interconnection, the following passivity condition should be held (assuming the initial energy at $t=0$ is zero):

$$\int_0^t f_p^*(\tau)^T \cdot v_p(\tau)\, d\tau \geq 0, \quad (20)$$

Considering (20) and the force decomposition (2), we have

$$\int_0^t f_p^*(\tau)^T \cdot v_p(\tau)\, d\tau = \int_0^t f_p(\tau)^T \cdot v_p(\tau)\, d\tau + \int_0^t f_{react}(\tau)^T \cdot v_p(\tau)\, d\tau. \quad (21)$$

As a result, the passivity condition for the entire system Σ_2 can be evaluated by the following passivity integral:

$$\int_0^t f_p(\tau)^T \cdot v_p(\tau)\, d\tau + \int_0^t f_{react}(\tau)^T \cdot v_p(\tau)\, d\tau \geq 0. \quad (22)$$

It can be seen from Fig. 4 that $\int_0^t f_{react}(\tau)^T \cdot v_p(\tau)\, d\tau$ is the *passivity integral of the patient's hand reaction dynamics* Σ_3 and $\int_0^t f_p(\tau)^T \cdot v_p(\tau)\, d\tau$ *is the passivity integral of the therapy terminal* Σ_1. Consequently, considering the passivity condition (22), **if the therapy terminal Σ_1 behaves as a nonpassive system, the entire system Σ_2 can still remain passive if the energy of patient hand's reaction dynamics, i.e. $\int_0^t f_{react}(\tau)^T \cdot v_p(\tau)\, d\tau$, can compensate for the energy injected by the therapy terminal**.

Considering the passivity condition (22) and the definition of L_2 stability given in Remark 3, when initial energy at $t=0$ is zero, we have

$$\text{the entire system } \Sigma_2 \text{ is } L_2 \text{ stable if } \exists\ \xi_r > 0 \text{ s.t. } \int_0^t f_p(\tau)^T \cdot v_p(\tau)\, d\tau + \int_0^t f_{react}(\tau)^T \cdot v_p(\tau)\, d\tau \geq \xi_r \cdot \int_0^t v_P(\tau)^T \cdot v_p(\tau)\, d\tau. \quad (23)$$

Consequently, if (23) is satisfied and the input energy provided to the entire system through f_p^* is bounded, the output energy of the entire system will remain bounded and the system Σ_2 will remain L_2 stable.

Let us consider an INP model for the therapy terminal impedance Σ_1 with shortage of passivity of $\hat{\delta}_{th} \leq 0$ as

$$\int_0^t f_p(\tau)^T \cdot v_p(\tau)\, d\tau \geq \hat{\delta}_{th} \cdot \int_0^t v_P(\tau)^T \cdot v_p(\tau)\, d\tau, \quad \text{s.t. } \hat{\delta}_{th} \leq 0, \quad (24)$$

and an OSP model for the patient reaction admittance Σ_3 with excess of passivity $\xi_p \geq 0$ as

$$\int_0^t f_{react}(\tau)^T \cdot v_p(\tau)\, d\tau \geq \xi_p \cdot \int_0^t v_P(\tau)^T \cdot v_p(\tau)\, d\tau, \quad \text{s.t. } \xi_p \geq 0. \quad (25)$$

Combining (23), (24), and (25) the following will result:

$$\text{the entire interconnection } \Sigma_2 \text{ is } L_2 \text{ stable if } (\xi_p + \hat{\delta}_{th} - \xi_r) \cdot \int_0^t v_P(\tau)^T \cdot v_p(\tau)\, d\tau \geq 0 \quad (26)$$

Considering (26) and a small positive arbitrary value ξ_r, the novel L_2 stability condition of the entire system Σ_2 is

$$\xi_p + \hat{\delta}_{th} - \xi_r \geq 0 \quad (27)$$

This validates Hypothesis I that is a new analysis of stability for haptics-enabled systems. It should be noted that in

(27), ξ_r is a tunable factor that defines a flexible stability margin for the system. Higher values for ξ_r provide a more conservative stability condition for the system which can be used if uncertainty in the system dynamics is considerable.

As a result, the entire system Σ_2 will remain L_2 stable with the stability margin ξ_r, if the EOP of the reaction dynamics of the patient's hand Σ_3 can compensate for the SOP of the therapy terminal Σ_1. The minimum required value for the EOP of the patient's limb is $\xi_p > |\xi_r| + |\hat{\delta}_{th}|$. If the above-mentioned condition is not satisfied, damping should be added to compensate only for the *extra energy* not dissipated by the EOP of the patient's limb. In the next section, the M-TDPC approach is proposed to stabilize the system, when the stability condition (27) is not met due to insufficient EOP. The approach, customizes the delivered therapeutic energy to achieve the performance goals.

Remark 4. Note that the EOP of a person's hand is the capabilities of his/her limb in absorbing the interactive energies, and is linked to the biomechanical characteristics of the corresponding limb. As a result, if a patient has a rigid or spastic hand with high muscular activity tone (a common symptom of stroke), he/she has a higher EOP compared to a patient with softer limbs. •

VI. Proposed Stabilizing Control Design: M-TDPC Scheme

In this section, the proposed control scheme is presented, which is capable of guaranteeing stability of the system when the stability condition (27) is not satisfied. The controller is a new member of the TDPC approach family and is named M-TDPC. The goal is to utilize the biomechanics of the patient's hand to enhance transparency while allowing the nonpassive assistive energy to flow and ensuring passivity and stability of the entire system. The philosophy of the proposed M-TDPC controller is to provide the minimum necessary damping injection, taking advantage of our knowledge about the EOP of the patient's hand, and is capable of eliminating just the extra energy while letting the therapist provide assistance to the patient. The proposed controller has two major components: (a) a Passivity Differential (PD) calculator, (b) a stabilizing core. The roles of the mentioned components are as follows.

A. Passivity Differential (PD) Calculator

This component of the controller is responsible to find the minimum amount of energy that results in deviation from stability condition (27) and needs to be dampened out. As a result, the PD calculator takes into account the EOP of the patient's limb and the SOP of the delivered therapy to calculate the minimum amount of energy to be dampened out that guarantees stability in the context of SPT. Considering (26) and (27), let us define

$$\begin{aligned} E_p(t) &:= (\xi_p - \xi_r) \cdot \int_0^t v_P(\tau)^T \cdot v_p(\tau)\, d\tau, \\ E_{th}(t) &:= \int_0^t f_P(\tau)^T \cdot v_p(\tau)\, d\tau, \end{aligned} \tag{28}$$

Based on (28), the PD can be calculated as

$$PD(t) := E_p(t) + E_{th}(t). \tag{29}$$

PD represents the difference between the energy that can be damp out by the user's limb, i.e. $E_p(t)$, and the energy delivered by the therapist through the communication network, i.e. $E_{th}(t)$. Based on the definition of PD given in (29), the Lack of Passivity (LOP) is defined as

$$LOP(t) = \begin{cases} 0 & if\ PD \geq 0 \\ PD & if\ PD < 0 \end{cases} \tag{30}$$

Considering (30), if the passivity of the patient's limb (E_p) can compensate for the nonpassivity of the therapy terminal ($|E_p| > |E_{th}|$), the $LOP(t)$ is zero. This is because in this situation, there is no need to compensate for any energy, even if the therapy terminal (combination of environment and communication) is nonpassive ($E_{th} \leq 0$). In addition to the above, $LOP(t)$ remains zero if the therapy terminal is passive ($E_{th} \geq 0$). However, if $E_p + E_{th} \leq 0$, which means that the EOP of the patient's limb is not capable of providing enough dissipation to compensate for the nonpassivity of the therapy terminal, the $LOP(t)$ will be equal to the differences between $|E_p|$ and $|E_{th}|$ and will have a negative sign. This defines the minimum energy required to be dampened out by the controller to keep the entire interconnection stable.

Remark 5. Considering (30), to calculate $PD(t)$ and $LOP(t)$, we need to have access to E_p and E_{th}. Based on the definitions given in (28), E_{th} is accessible in real-time since both v_p and f_p are measurable. However, this is not the case for E_p. In fact, E_p is a property of the dynamics of the patient's limb and is a function of ξ_p, which is directly related to f_{react} as can be seen in (25). f_{react} is not directly accessible in real-time since (2) is an undetermined equation. As a result, the question is: *"how to identify the excess of passivity of the patient's hand in order to calculate $PD(t)$?"*. In order to deal with this issue, we have proposed an identification technique for ξ_p, as given in the next subsection.

EOP Identifier for the Patient's Hand :

As mentioned, there is no direct way to quantify the EOP of the reaction dynamics of the patient's limb, i.e., ξ_p, and passivity integral $\int_0^t f_{react}(\tau)^T \cdot v_p(\tau)\, d\tau$, during task performance, when the operator is applying f_p^*. The aforementioned issue arises since the only measurable component of the force decomposition (2) is f_p. Consequently, $f_{react}(t)$ is not accessible when the exogenous force $f_p^*(t)$ in (2) is not zero. As a result, during rehabilitation tasks, since patient is applying f_p^*, it is not possible to calculate ξ_p. In this part, an identification scheme is proposed to *estimate* the EOP for the reaction dynamics of the patient's limb that can be used in the proposed PD calculator (29).

For this purpose, an off-line identification scheme is used before the start of the therapy. This allows us to estimate ξ_p for each patient in order to customize the allowed therapeutic energy for him/her during the therapy. As a result, the proposed technique will be able to distinguish between a patient with rigid limbs versus a one who has compliment limbs. To achieve the above-mentioned goal, during the

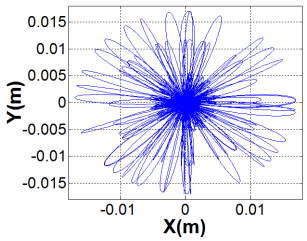

Fig. 5. The planar 2D trajectories used for hand perturbation during the EOP identification procedure.

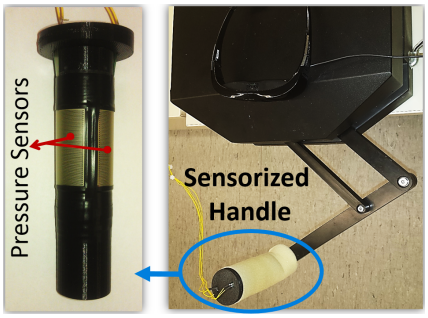

Fig. 6. The sensorized handle connected to the rehabilitation device

identification phase (before the start of therapy), the patient is asked to hold the robotic handle in a "relaxed" condition and let the robot perturb her/his hand. ***The definition of the relaxed condition and why this condition is considered will be detailed later in Remarks 7 and 8***. The robot provides movements of different frequencies/trajectories while recording motion and force information.

Since during identification procedure the patient is not asked to track any trajectory, he/she does not apply exogenous forces: $f_p^* = 0$. Consequently, during the identification procedure, $\int_0^t f_{react}(\tau)^T \cdot v_P(\tau)\, d\tau = \int_0^t f_p(\tau)^T \cdot v_P(\tau)\, d\tau$, while both $f_p(t)$ and $v_p(t)$ are measured. As a result, based on (25) and using the collected data from the identification phase, the estimated EOP for the patient's limb in the relaxed condition can be calculated as

$$\xi_{p-relax} = \frac{\int_0^{T_e} f_{react}(\tau)^T \cdot v_P(\tau)\, d\tau}{\int_0^{T_e} v_p(\tau)^T \cdot v_P(\tau)\, d\tau} \tag{31}$$

In (31), $\xi_{p-relax}$ is the estimated EOP for the patient's limb in the relaxed condition and T_e is the duration of identification procedure. Then during the rehabilitation phase, $\xi_{p-relax}$ is used in (28),(29) and (30) to calculate $PD(t)$ and $LOP(t)$. For this purpose, after estimating $\xi_{p-relax}$ for each patient, $PD(t)$ and $LOP(t)$ are calculated as

$$LOP(t) = \begin{cases} 0 & if\ PD \geq 0 \\ PD & if\ PD < 0 \end{cases} \tag{32}$$

$$\begin{aligned} &\text{where} \quad PD(t) := E_{p-relax}(t) + E_{th}(t), \\ &E_{p-relax}(t) := (\xi_{p-relax} - \xi_r) \cdot \int_0^t v_P(\tau)^T \cdot v_p(\tau)\, d\tau \end{aligned} \tag{33}$$

In (33), $v_p(t)$ is the real-time measurment of the patient's hand velocity during the rehabilitation phase and $\xi_{p-relax}$ is the EOP of the patient's limb in the relaxed condition and as identified during the identification phase.

Remark 6. In this work, two degrees of freedom (DOF) horizontal Cartesian perturbation is considered for the identification phase. The user's limb is perturbed for 60 second, using a stimulation trajectory that is a summation of ten sinusoidal, in the range $0-3Hz$ (to cover rehabilitation requirements) with a maximum amplitude of 1.5 cm. The perturbation signal is shown in Fig 5. •

Remark 7. The reason that the relaxed condition of the limb is considered in the identification procedure for the EOP is that the patient may vary the properties of his/her grasp during the rehabilitation phase. As a result, he/she may provide a rigid grasp at some time episodes while providing a loose grasp at some others. We need to make sure that the system performs appropriately in any condition. Consequently, we have considered the minimum EOP that can be delivered by the operator to find the minimum energy that can be observed by the patient's limb. The minimum ξ_p happens in the relaxed condition, when the patient grasp the robotic handle in a relaxed manner. For consistency and to make sure that the patient remains in the relaxed condition, during the identification phase, a sensorized handle is constructed and connected to the end-effector of the rehabilitation robot as shown in Fig. 6. The relaxed condition is defined as when the grasp pressure is at a very low value (between $2\%-5\%$ of the user's maximum achievable grasp pressure). The mentioned range is monitored to the patient (using a head-mounted display) and the patient is asked to keep the grasp pressure within the monitored range regardless of the motion of the robot, during the identification phase. •

Remark 8. To illustrate the effect of grasp pressure on ξ_p, we have calculated the EOP for a healthy participant under an ethics approval from the University of Alberta Research Ethics Board (Study ID: Pro00033955). We have tested ξ_p in two conditions: (a) relaxed condition defined above to calculate $\xi_{p-relax}$, and (b) rigid grasp condition (when the participant is asked to keep the pressure between $75\%-85\%$ of the maximum pressure during identification) to calculate $\xi_{p-rigid}$. It is observed that increasing the grasp pressure increases the EOP of the hand to more than 400% of that in the relaxed condition (from 5.56 $N.s/m$ for $\xi_{p-relax}$ to 25.06 $N.s/m$ for $\xi_{p-rigid}$). In summary, $\xi_{p-relax}$ is the lower-bound for the possible EOP delivered by the patient during rehabilitation and can define the minimum energy that can be observed by the user during task execution. That is why it is considered in (33) to ensure stability for all possible grasp conditions. •

B. Stabilizing core

The second component of the controller is responsible to compensate for the calculated the nonpassive energy which cannot be absorbed by the EOP of the patient's limb.

In the literature, compensating for energy is done in TDPC approach [20],[21],[22],[37]. We will use the similar

concept to meet the stability condition (22). This enables customizing the therapeutic energy based on the biomechanical capabilities of the patient's limb (specifically EOP of the limb). Consequently, for a patient with high EOP value of his/her limb that can absorb more therapeutic energy, the proposed controller allows more assistive energy to be delivered compared to a patient with low EOP value.

Such as all TDPC approaches (e.g., [37]) compensating for energy is done through injecting time-varying damping $\alpha(t)$ into the system, considering the derivative of the energy. The aforementioned derivative is $\frac{d}{dt}PD(t)$ in this work and is defined by $P_L(t)$ as

$$P_L(t) = \frac{d}{dt}PD(t). \tag{34}$$

Considering the time stamp n for the current sample of signals, the proposed M-TDPC is formulated as

$$f_{th-mod}(n) = \hat{f_{th}}(n) + \alpha(n) \cdot v_p(n) \tag{35}$$

$$\text{where } \alpha(n) = \begin{cases} \frac{-LOP_{obs}(n)}{\Delta T\left(v_p(n)^T \cdot v_p(n)\right)} & \text{if } LOP_{obs}(n) \leq 0 \\ 0 & \text{if } LOP_{obs}(n) \geq 0, \end{cases} \tag{36}$$

$$\text{and } \; LOP_{obs}(n) = LOP_{obs}(n-1) + [P_L(n) + \alpha(n-1)v_p(n-1)^T \cdot v_p(n-1)]\Delta T. \tag{37}$$

In (35), (36) and (37), ΔT is the sampling period, α is the designed time-varying damping implemented on the patient's side, f_{th-mod} is the modified force to be reflect to the patient's hand, LOP_{obs} is the output of the energy observer (37). The details regarding the stabilizing behavior of the controller is given in the appendix.

Up to this point, we have the stabilizer which is developed based on the new definition of system passivity which considers the effect of the biomechanical features of the operator's hand and allow for delivering customized nonpassive energy. In the next step a new way of further enhancing the performance of the stabilizer is proposed.

C. Performance Enhancement

One of the challenges of TDPC-based techniques is potential lagged diagnosis of nonpassivity, which may ultimately result in sudden change and large control forces. In fact, when an interconnection remains passive for a relatively long period of time, the passive energy will be accumulated in the energy reservoir of the observer. Consequently, if at some point the behavior of the interconnection changes to a nonpassive one, it may take some time for the energy observer to recognize the nonpassivity. When the nonpassivity is observed, the controller will try to compensate as quickly as possible, which can result in the mentioned behavior of the control signal. This behavior could be oscillations or sudden increase of the force input. This has been studied in the literature. For the case of rehabilitation, this situation should be analyzed and addressed exclusively as the therapist may frequently switch from resistive to assistive therapy, and vice versa.

In the literature, to deal with the aforementioned issue, the Power-domain TDPC (PTDPC) has been developed [38], [39]. The PTDPC observes the power instead of energy. Once the technique observes a negative power packet, which may challenge the passivity, it provides damping to cancel out the packet. Although this technique distributes the damping on a larger period of time, makes the control signal smoother compared to energy-domain TDPC, and resolves the issue of energy accumulation in the observer's reservoir, it may degrade the performance [39] since it does not allow any negative power packet to flow and does not consider any part of the history of the system's energy.

Remark 9. It should be noted that the proposed M-TDPC approach given in (35), (36), (37) works in the energy domain. It is possible to develop the power-domain version of the M-TDPC approach (as explained in the remaining of this section). However, if we develop the power-domain version of the proposed M-TDPC approach, when the therapist switches from passive behavior to nonpassive behavior, the power-domain version is more conservative than the energy-domain one (since it quickly starts dampening the energy of the system). However, when the behavior switches from nonpassive to passive, the energy-domain version is more conservative than the power-domain one (since it continues to dampening the energy for a period of time while the interconnection has already became passive). Consequently, both designs may have some advantages and disadvantages in the context of rehabilitation since the therapist may provide a mixed variation of resistive and assistive energies during therapy. •

To address the raised concern, the corresponding design of the M-TDPC technique given in (35)-(37) is enhanced using a new definition of energy function, entitled Windowed Energy (WE). The goal of the proposed enhancement is to consider a sliding weighted time window to calculate the energy, and provide damping if the energy of the considered window is nonpassive. The enhanced M-TDPC approach is given in (38)-(40), wherein the main difference from the original design is applying the concept of WE by adding Γ_w in the observer's formulation (40).

$$f_{th-mod}(n) = \hat{f_{th}}(n) + \alpha(n) \cdot v_p(n) \tag{38}$$

$$\text{where } \alpha(n) = \begin{cases} \frac{-LOP_{obs}(n)}{\Delta T\left(v_p(n)^T \cdot v_p(n)\right)} & \text{if } LOP_{obs}(n) \leq 0 \\ 0 & \text{if } LOP_{obs}(n) \geq 0, \end{cases} \tag{39}$$

$$LOP_{obs}(n) = \Gamma_w \cdot LOP_{obs}(n-1) + [P_L(n) + \Gamma_w \cdot \alpha(n-1)v_p(n-1)^T \cdot v_p(n-1)]\Delta T \;\; , \;\; 0 \leq \Gamma_w \leq 1. \tag{40}$$

Considering (40), if Γ_w is equal to unity, the technique will convert to the energy-domain M-TDPC technique given in (35), (36), (37). If Γ_w is equal to zero, the technique will convert to the power-domain version of the M-TDPC approach (which just accounts for power packets and not the history of the system energy). Considering an Γ_w value between zero and unity acts as a forgetting factor for the dynamics of the observer and provides very small weights for the early power packets and higher weights for the recent packets. Tuning the Γ_w value can change the effective width of the window (memory of the observer). In other words, for $0 < \Gamma_w < 1$, the M-TDPC approach

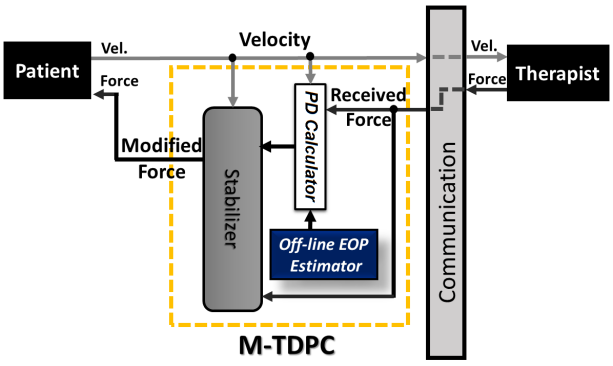

Fig. 7. The resulting interconnection.

acts quicker than the energy-domain version of it (to avoid energy accumulation issue) and slower than power-domain version. Consequently, by using $0 < \Gamma_w < 1$ (a) the behavior of the therapist in the very early periods of therapy will not change the decision on modifying therapeutic forces for later stages of procedure, (b) the controller does not eliminate all negative power packets and still considers a windowed history of the delivered therapeutic energy.

A schematic of the interaction including the stabilizer, PD calculator, and EOP estimator is shown in Fig. 7.

VII. Simulation Results

In this section results of some numeric simulations are given to evaluate the performance of the stability analysis technique and the proposed controller. For this purpose two sets of simulations are presented, as follows.

A. Simulation I: Stability Analysis

In the first simulation, the derived stability condition (27) is evaluated. For this purpose PAT is simulated under communication delays. The SOP of the therapy is considered to be lower than the EOP of the operator for the first phase of the simulation (entitled mild assistance) and then it is considered to be higher than the EOP for the second phase (entitled strong assistance). No controller is applied to evaluate the proposed stability condition. It is expected that when the stability condition (27) is satisfied (the first phase) the entire system remains stable (though the therapy terminal is nonpassive due to the communication delay and the assistive behavior of the simulated therapist). Also, we expect that when the stability condition is not satisfied (the second phase) the entire system becomes unstable. The simulation parameters are given in Table I, where the EOP of the patient's hand and the SOP of the therapies, in both phases, have been calculated using the identification technique defined in the previous section. During both phases, the therapies start from $t = 30$. If the assistance is delivered the amplitude of velocity trajectories should become larger. For the first phase, the results of the velocity tracking and force tracking can be seen in Figs. 8(a) and 8(b), respectively. As can be seen in Figs. 8(a) and 8(b), during mild assistance phase, since

TABLE I
The Simulation Parameters

Master Robot Dynamics	$Z_m(s) = \frac{V_m(s)}{F_m(s)} = \frac{1}{2s+2}$
Patient's hand Dynamics	$Z_p(s) = \frac{V_p(s)}{F_p(s)} = \frac{1}{s+8}$
Therapist's PAT Gain	First phase: $D_{th} = 4$, Second phase: $D_{th} = 16$
Communication Delay	$\tau_1(t) = \tau_2(t) = 80 + 10sin(\frac{\pi}{4}t)$ ms
Exogenous Input	$f_p^*(t) = 2\big(sin(0.5t) + sin(t) - sin(1.5t) - sin(2t)\big)$
Sampling Time	$\Delta T = 0.01\ s$
EOP of the Patient's limb	$\xi_p = 8.05$
SOP of the delivered therapy	The first phase: $\hat{\delta}_{th} = -3.92$ The second phase: $\hat{\delta}_{th} = -15.67$

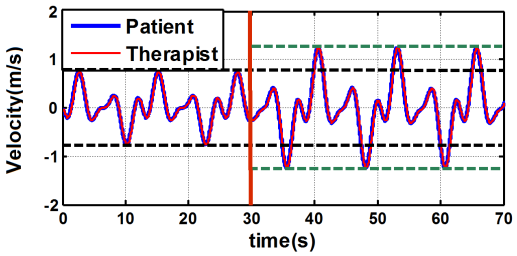

(a)

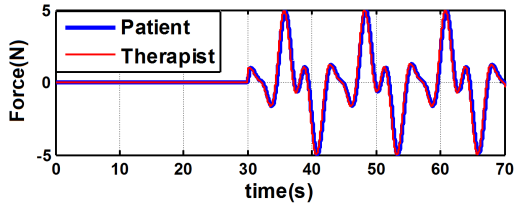

(b)

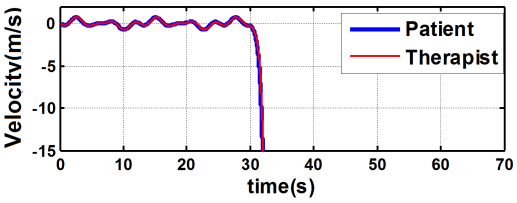

(c)

Fig. 8. (a) Velocity tracking for the case of assistive therapy, when the stability condition is satisfied, (b) Force tracking for the case of assistive therapy, when the stability condition is satisfied, (c) Velocity tracking for the case of assistive therapy, when the stability condition is not satisfied.

the stability condition (27) is satisfied, the entire system behaves in a stable manner. The velocity tracking and the force tracking results follow (11) and (12). In addition, the amplitude of the velocity trajectories are amplified due to the delivered assistive energy. The next step is to simulate the strong assistance phase when there is no controller. The corresponding velocity tracking result for the second phase is given in Fig. 8(c) As can be seen in Fig. 8(c), during strong assistance, since the stability condition (27) is not satisfied and no controller is applied, the interconnection becomes unstable and the trajectories grow in an unbounded manner. This shows the necessity of having a stabilizer.

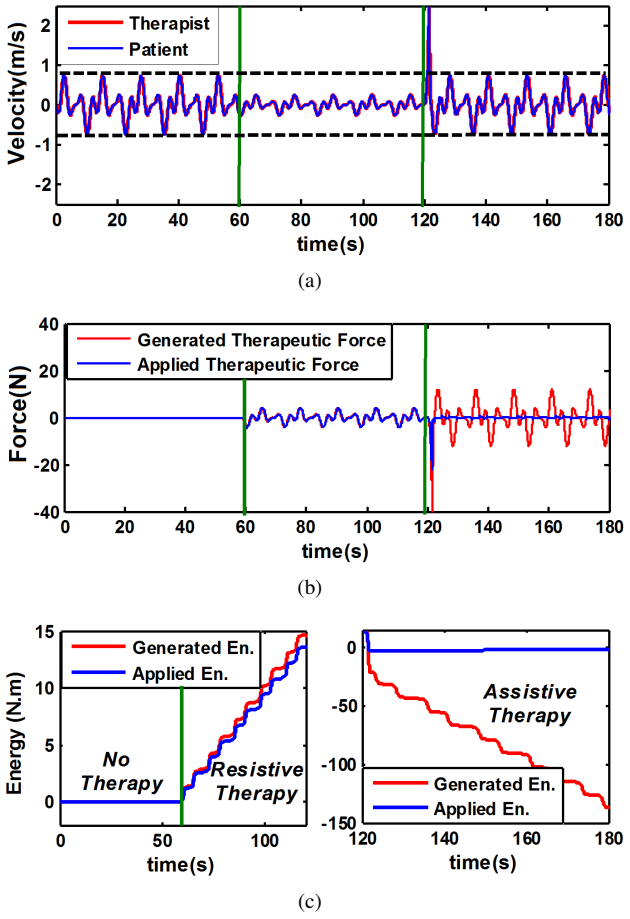

Fig. 9. The simulation results for applying TDPC approach for resistive therapy ($60 < t < 120$) and assistive therapy ($120 < t < 180$), (a) Velocity tracking, (b) Force Modulation, and (c) Energy Modulation.

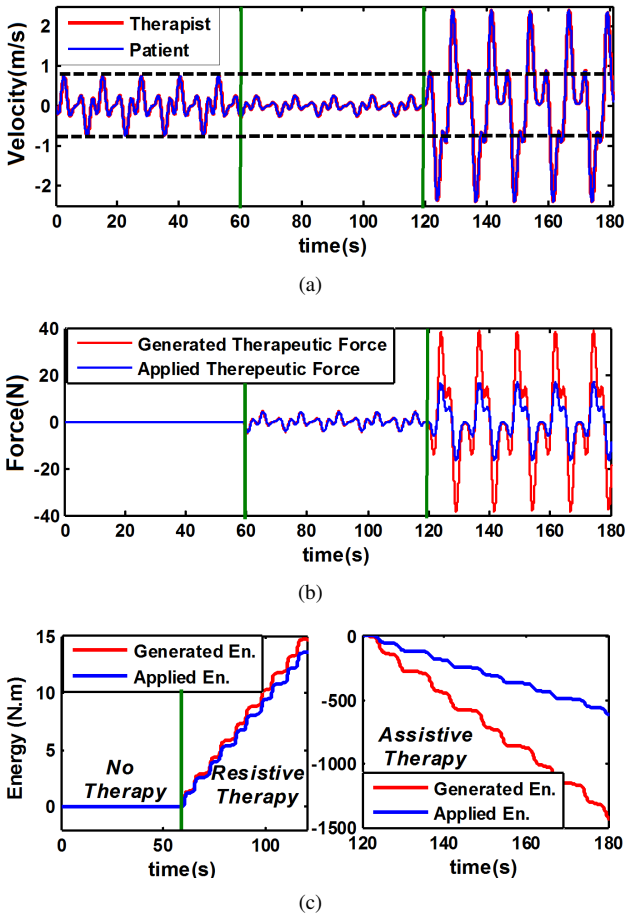

Fig. 10. The simulation results for applying M-TDPC approach for resistive therapy ($60 < t < 120$) and assistive therapy ($120 < t < 180$), (a) Velocity tracking, (b) Force Modulation, and (c) Energy Modulation.

B. Simulation II: M-TDPC stabilizer

In this part, the performance of the propose M-TDPC is analyzed. For this purpose, in addition to the proposed controller, the original One-port TDPC is simulated (and named TDPC throughout the simulation). The One-port TDPC approach composed of an observer and a controller on the master side to compensate for nonpassivity of Σ_1. Both of the simulated controllers can be applied even when the communication delay is zero. In fact, this simulation focuses on the effects of considering the EOP of the patient's hand in the design of the TDPC-based stabilizers. The simulation conditions are the same for both controllers. For this goal, the total simulation time is considered to be $180s$. In addition, for M-TDPC approach, Γ_w and ξ_r are considered to be 0.7 and 1.05, respectively. During the first 60 seconds no therapy is applied, then the resistive therapy is started considering $D_{th} = -16$, till $t = 120s$. Afterwards, the therapy is switched to strong assistance ($D_{th} = 16$). Other simulation parameters are similar to that of Simulation I. The corresponding results (velocity tracking, force tracking and energy modulation) for the cases of One-port TDPC and M-TDPC are given in Figs. 9 and 10, respectively. As can be seen in Fig. 9(a), using the TDPC approach, during the resistive phase ($60 < t < 120$), the amplitude of the velocity trajectories have been reduced in comparison to that of the no-therapy phase ($0 < t < 60$). This means that the resistive behavior is delivered, which is the goal of the therapy. Also, the TDPC technique is not considerably changing the reflected forces during resistive therapy (as in Fig. 9(b)). In Fig. 9(c), left part, the generated resistive energy at the therapist's side is compared to the applied energy to the patient's hand, during $60 < t < 120$. The corresponding slight difference between the energies is due to the communication delay. In other words, the TDPC approach has delivered most of the resistive energy.

However, in contrast to the resistive phase of the simulation, during the assistive phase ($120 < t < 180$), the therapy is not delivered using the One-port TDPC. This can be seen in Fig. 9(a), where the velocity trajectories have not become larger, in Fig. 9(b), where the applied force is almost zero, and in Fig. 9(c) (the right figure), where the applied energy is flattened. This problem is due to the fact that the One-port TDPC approach assumed that the assistive energy is not desirable and should be dampened out.

Note that the overshoot at $t = 120s$ is due to the energy accumulation in the observer reservoir that has been discussed in the previous section. This overshoot is excluded from the result analysis, in this simulation, but is exclusively studied in Simulation III.

Considering Fig. 10, during the resistive phase of the

TABLE II
FORCE REFLECTION RATIO

	M-TDPC	TDPC
Resistive Therapy	$FRR = 98.83\%$	$FRR = 98.92\%$
Assistive Therapy	$FRR = 43.88\%$	$FRR = 1.2\%$
$\textbf{Force Reflection Ratio}(FRR) = \frac{mean(\lvert f_{th-mod}\rvert)}{mean(\lvert f_{th}\rvert)}$		

simulation $60 < t < 120$ the behavior of the propose M-TDPC approach is similar to that of the TDPC technique in Fig. 9. This means that the M-TDPC approach is also able to deliver resistance over communication delays, in a similar manner to one-port TDPC approach. However, using the proposed M-TDPC approach it is possible to deliver assistive energy, and simultaneously guaranteeing the interconnection stability. This fact can be seen during $120 < t < 180$ in Fig. 10(a), where the amplitude of the velocity trajectory is considerably amplified, in Fig. 10(b) where the amplitude of the assistive force is not zero, and in Fig. 10(c) where the applied assistive energy to the patient's hand is not flattened while the system is behaving in a stable manner. Considering Figs. 10(b) and 10(c) the force/energy modulation performed by the M-TDPC technique can be observed. In fact, the proposed controller has modified the applied energy to the patient's hand (in comparison with the generated energy), based the capabilities of the patient's limb in absorbing/dissipating the nonpassive therapeutic energy. As given in Table I, the identified EOP of the simulated user is 8.05; considering $\xi_r = 1.05$ the proposed controller is able to guarantee the stability of the system while allowing the nonpassive energy to flow.

In Fig. 11, the distribution of the absolute value of the velocities during the no-therapy phase, the assistive therapy phase and the resistive therapy phase have been shown for the cases of M-TDPC approach (Case #1) and the simulated One-port TDPC approach (Case #2). Based on Fig. 11, using the M-TDPC approach, the resulting velocities during assistance is considerably higher than that of the no-therapy phase. However, this is not the case for the other approach.

In addition, the Force Reflection Ratio (FRR) is defined in Table II. FRR is the ratio between the mean value of the modified forces over the mean value of the generated therapeutic forces. For resistive therapy, both M-TDPC and TDPC approaches were able to deliver most of the generated forces. The slight deviation from ideal 100% reflection is due to the behaviors of the controllers in dealing with the existing delays. Using the M-TDPC approach, for the case of assistive therapy, the FRR is 43.88% which interestingly is close to $(\xi_p - \xi_r)/\hat{\delta}_{th}$. It tells that the higher the EOP of the patient's limb, the more assistive forces can be reflected to the patient's hand through the M-TDPC approach. However, for the case of TDPC technique (during assistive phase) the FRR is small, which tells that the technique is not capable of delivering assistance and it cancels out the assistive forces.

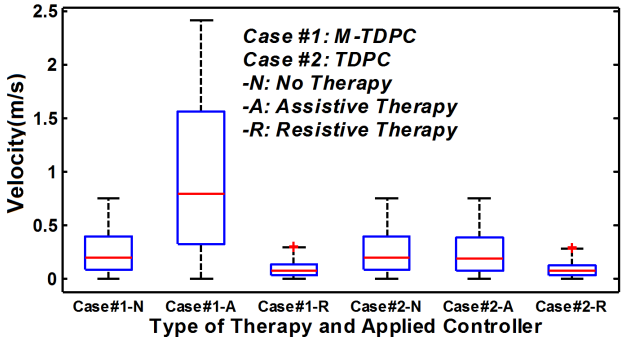

Fig. 11. Velocity tracking for the case of assistive therapy, when the stability condition is not satisfied

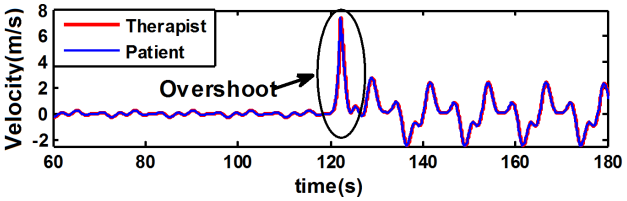

(a)

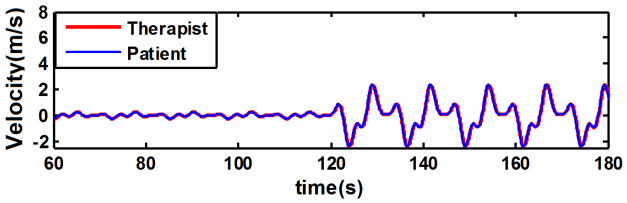

(b)

Fig. 12. The velocity tracking using the proposed M-TDPC approach, (a) $\Gamma_w = 1$, (b) $\Gamma_w = 0.7$.

C. Simulation III: The Effect of Γ_w

In this simulation, the effect of Γ_w is analyzed. For this purpose the simulation condition is considered similar to Simulation II. The performance of the proposed M-TDPC approach is evaluated considering $\Gamma_w = 1$ and $\Gamma_w = 0.7$. The corresponding results are given in Fig. 12. As can be seen in Fig. 12(a), when $\Gamma_w = 1$ the velocity trajectory has a overshoot of 296%. This is due to the fact that with $\Gamma_w = 1$ the width of the considered window of the energy reservoir in the observer is infinity. Consequently, the accumulated energy during the entire resistive phase ($60 < t < 120$) results in late detection of nonpassive therapy. As a result, the velocity trajectories suddenly increase when the task switches from a resistive one to an assistive one. This issue is resolved using the concept of WE by considering $\Gamma_w = 0.7$, as can be seen in Fig. 12(b).

VIII. EXPERIMENTAL EVALUATION

In this section, experimental results are provided to support the proposed M-TDPC approach for an implementation of the HTR system. The setup consists of the following:
(A) Master robot at the patient's side: This is a 2-DOF planar upper-limb rehabilitation device from Quanser Inc. (Markham, ON, Canada) that moves in the horizontal (X-Y) plane allowing for arm flexion-extension. The robot is

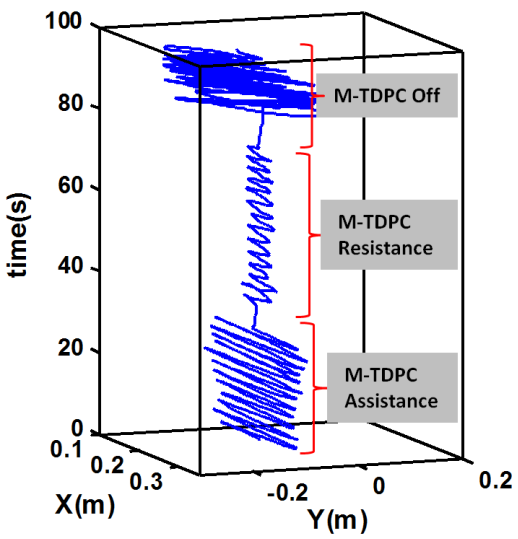

Fig. 13. Motion trajectories of the patient during resistive and assistive therapy when the controller is ON compared to the behavior of the system when the controller is OFF

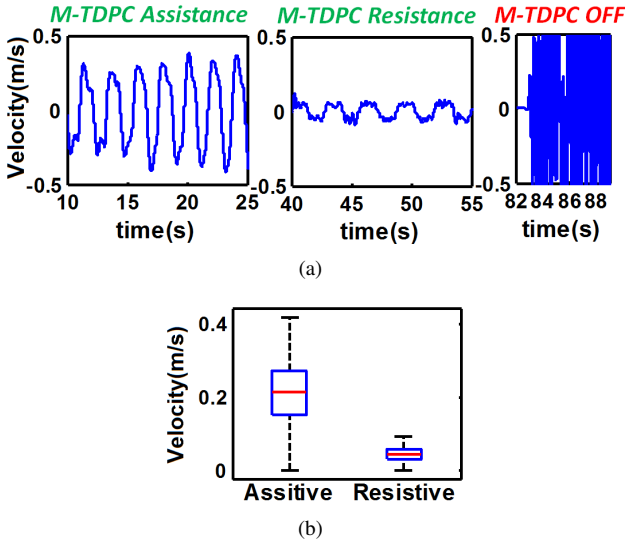

Fig. 14. (a) Velocity trajectory, (b) Velocity distribution for 20 seconds of assistive and resistive therapies.

shown in Fig. 1 and Fig. 6. The handle of the robot was sensorized (Fig. 6) using two pressure sensors.

(B) Slave robot: This is a 6-DOF Quanser HD^2 haptic device locked in 4 degrees of freedom using software to provide a similar workspace to that of the master robot.

(C) Virtual Environment (VE): This is shown in Figs. 2 and 1. The VE was developed in C++ and communicates with the robots through the UDP protocol. A head-mounted display (shown in Fig. 1) is used at the patient's side to represent the VE and provide visual cues.

A. Experimental Scenario and Results

In this experiment, the first operator, who played the role of the patient, tried to track the green target in the VE. The second operator, who played the role of the therapist, applied assistive forces during the first phase, and then resistive forces during the second phase, while the M-TDPC controller was ON. The controller was turned off in the third phase. The communication delay was $\tau_1 = \tau_2 = 80 + 10\ sin(\frac{\pi}{4}t)\ ms$. The EOP of the operator's hand was identified as $\xi_{p-relax} = 5.56$. In addition, we have $\xi_r = 0.56$ and $\Gamma_w = 0.7$. The goal was to evaluate the behavior of the M-TDPC approach in addressing resistive and assistive environments.

In the VE, the target switched every 1 second between two locations along the vertical axis (X direction). The first operator was asked to keep the effort as consistent as possible during both phases. The result of the tracking should be vertical trajectories. The switching time was considered small to challenge the operator, playing the role of the patient. The position tracking result is shown in Fig. 13. As can be seen, the amplitudes of the generated motion for the case of assistive therapy were increased in comparison to that of the resistive phase. For the resistive phase, the first operator was not able to reach the targets within the 1-second time window since the second operator was resisting him. The system became unstable once the controller was turned off. This resulted in uncoordinated motions in both the X and Y directions. The velocity tracking result is shown in Figs. 14(a) and 14(b). As can be seen in Fig. 14(a), the amplitude of the velocity trajectory during assistive phase was considerably higher than that of the resistive phase and the system was able to properly deliver both types of actions. It quickly became unstable once the controller was turned off. Fig. 14(b) shows the distribution of the absolute values of the velocity trajectories for 20 seconds of assistive therapy versus resistive therapy. The mean value for the assistive phase was 0.2095 m/s and for the resistive phase was 0.043 m/s. Using statistical analysis (two-sample t-test) a *p-value* of 0.00014 was obtained which means that the difference between the two mean values was statistically significant.

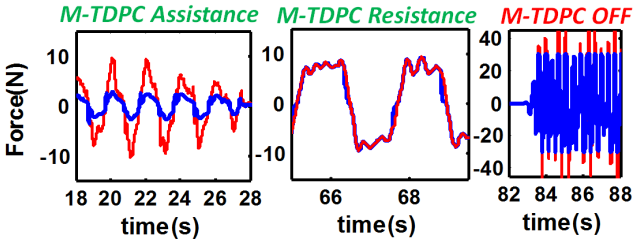

Fig. 15. The modified therapeutic forces (solid blue line), versus the delivered forces (solid red line)

To analyze the behavior of the controller, the modified and received therapeutic forces were monitored, as well. Note that force saturation of $30N$ was also used. The result can be seen in Fig. 15. As can be seen, during the assistive therapy, the controller was capable of detecting the nonpassive nature of the therapy; as a result, it modified the therapeutic forces (based on the identified $\xi_{p-relax}$) before reflecting them to the hand of the operator. Although the nature of the therapy was assistive (in the first phase), the controller allowed for assistive forces to be delivered in a modified manner (which was compatible with the biome-

chanical capabilities of the user's limb), while preserving stability. Note that if the operator had a higher $\xi_{p-relax}$ or if the therapist had applied milder assistive forces, the required force modification would be less. Here, the second operator tried to apply high assistive forces to highlight the behavior of the controller. During the resistive therapy, since the nature of the therapy was passive, the controller did not considerably modify the forces (as expected). The slight modification during resistance was due to the existence of the communication delay. During the third phase, when the controller was turned off, the system became unstable. This can be seen as high-frequency uncoordinated high-amplitude oscillations. In summary, the experimental results support the effectiveness of the developed theory and functionality of the proposed stabilizer (i.e. M-TDPC).

IX. CONCLUSION

In this paper, the stability of haptics-enabled robotic/ telerobotic rehabilitation systems was mathematically analyzed in the context of strong passivity theory to ensure safe patient-robot interaction. The proposed controller named M-TDPC which is a new member of the family of state-of-the-art TDPC controllers. The focus was to take advantage of the quantifiable EOP of the user's hand to guarantee interconnection stability. The proposed M-TDPC stabilizer allows the therapist to deliver nonpassive assistance over a delayed communication channel, based on the biomechanical capabilities of the patient's hand. The results in this paper can be extended for any general haptics-enabled robotic/telerobotic systems to also deal with delay-induced instability. The proposed M-TDPC controller increases the transparency of haptics-enabled systems since it does not require the modification of reflected forces if the EOP of the user's limb can compensate for the non-passivity in the system. In addition, based on the strong passivity theorem, the proposed stability analysis technique shows that under some specific conditions, the system can still remain stable without modifying the transparency, even if the communication system is exposed to variable time-delays. It should be noted that there is no assumption about the linearity and time-invariance of the therapist and the patient models. A simulation study and an experimental evaluation were conducted to validate the proposed theory.

APPENDIX

To show how the proposed controller guarantees stability of the system, considering (33) and (34), we have:

$$P_L(t) = (\xi_{p-relax} - \xi_r) v_P(t)^T v_p(t) + f_P(t)^T v_p(t) \tag{41}$$

$$\text{and } \sum_{k=0}^{n} P_L(k) = \sum_{k=0}^{n} (\xi_{p-relax} - \xi_r) v_P(k)^T v_p(k) + \sum_{k=0}^{n} f_P(k)^T v_p(k). \tag{42}$$

Let us define $W(n) = \frac{1}{\Delta T} LOP_{obs}(n)$. Considering (37), we have:

$$W(n) = \sum_{k=0}^{n} P_L(k) + \sum_{k=0}^{n-1} \alpha(k) v_P(k)^T v_p(k). \tag{43}$$

Now consider the passivity condition (22); in the presence of the controller (variable damping), the condition can be rewritten as

$$\Psi \geq 0 \text{ where } \Psi = \sum_{k=0}^{n} f_P(k)^T v_p(k) + \sum_{k=0}^{n} f_{react}(k)^T v_p(k) + \sum_{k=0}^{n} \alpha(k) v_P(k)^T v_p(k). \tag{44}$$

For Ψ we have:

$$\Psi = \sum_{k=0}^{n} f_P(k)^T v_p(k) + \sum_{k=0}^{n} f_{react}(k)^T v_p(k) + \Big(\sum_{k=0}^{n-1} \alpha(k) v_P(k)^T v_p(k) \Big) + \alpha(n) v_P(n)^T v_p(n). \tag{45}$$

Considering the definition of EOP, we have $\Psi > \hat{\Psi}$ where

$$\hat{\Psi} = \sum_{k=0}^{n} f_P(k)^T v_p(k) + \sum_{k=0}^{n} (\xi_{p-relax} - \xi_r) v_p(k)^T v_p(k) + \Big(\sum_{k=0}^{n-1} \alpha(k) v_P(k)^T v_p(k) \Big) + \alpha(n) v_P(n)^T v_p(n). \tag{46}$$

Combining (42),(43) and (46), we get:

$$\Psi > \hat{\Psi} \text{ where } \hat{\Psi} = W(n) + \alpha(n) v_P(n)^T v_p(n). \tag{47}$$

Considering (47) and the definition of $W(n)$, we have:

$$\Psi > \hat{\Psi} \text{ where } \hat{\Psi} = \frac{1}{\Delta T} LOP_{obs}(n) + \alpha(n) v_P(n)^T v_p(n). \tag{48}$$

Combining the design of the stabilizer given in (36), and the relation (48), the stability condition (44) is validated.

REFERENCES

[1] S. F. Atashzar, T. M. Shahbazi, Mahya, and R. V. Patel, "A new control technique for safe patient-robot interaction in haptics-enabled rehabilitation systems," in *IEEE/RSJ Int. Conf. on Intelligent Robots and Systems, (IROS 2015)*, 2015, pp. 4556–4560.

[2] D. Mukherjee and C. G. Patil, "Epidemiology and the global burden of stroke," *World neurosurgery*, vol. 76, no. 6, pp. S85–S90, 2011.

[3] W. H. Organization, "Global burden of stroke 15," *Stroke*, vol. 25.

[4] U. N. D. of International Economic, *et al.*, *World Population Ageing, 2013*, 2013.

[5] A. Butler, *et al.*, "Expanding tele-rehabilitation of stroke through in-home robot-assisted therapy," *Int J Phys Med Rehabil*, vol. 2, no. 184, p. 2, 2014.

[6] M. A. Dimyan and L. G. Cohen, "Neuroplasticity in the context of motor rehabilitation after stroke," *Nature Reviews Neurology*, vol. 7, no. 2, pp. 76–85, 2011.

[7] N. Takeuchi and S.-I. Izumi, "Rehabilitation with poststroke motor recovery: a review with a focus on neural plasticity," *Stroke research and treatment*, vol. 2013, 2013.

[8] H. I. Krebs and N. Hogan, "Therapeutic robotics: A technology push," *Proceedings of the IEEE*, vol. 94, no. 9, pp. 1727–1738, 2006.

[9] H. Kim, *et al.*, "Kinematic data analysis for post-stroke patients following bilateral versus unilateral rehabilitation with an upper limb wearable robotic system," *IEEE Trans. on Neural Systems and Rehabilitation Engineering*, vol. 21, no. 2, pp. 153–164, 2013.

[10] N. Hogan, *et al.*, "Motions or muscles? some behavioral factors underlying robotic assistance of motor recovery," *Journal of rehab research and development*, vol. 43, no. 5, pp. 605–618, 2006.

[11] *http://interactive-motion.com/healthcarereform/technology/*.

[12] O. Barzilay and A. Wolf, "Adaptive rehabilitation games," *J. of Electromyography and Kinesiology*, vol. 23, no. 1, pp. 182 – 189, 2013.

[13] E. Vergaro, *et al.*, "Self-adaptive robot training of stroke survivors for continuous tracking movements," *Journal of neuroengineering and rehabilitation*, vol. 7, no. 13, pp. 1–12, 2010.

[14] H. I. Krebs, *et al.*, "Rehabilitation robotics: Performance-based progressive robot-assisted therapy," *Autonomous Robots*, vol. 15, no. 1, pp. 7–20, 2003.
[15] S. F. Atashzar, *et al.*, "Networked teleoperation with non-passive environment: Application to tele-rehabilitation," in *IEEE/RSJ Int. Conf. on Intelligent Robots and Systems*, 2012, pp. 5125–5130.
[16] S. F. Atashzar, *et al.*, "Projection-based force reflection algorithms for teleoperated rehabilitation therapy," in *IEEE/RSJ International Conference on Intelligent Robots and Systems*, 2013, pp. 477–482.
[17] L. H. Schwamm, *et al.*, "A review of the evidence for the use of telemedicine within stroke systems of care a scientific statement from the american heart association/american stroke association," *Stroke*, vol. 40, no. 7, pp. 2616–2634, 2009.
[18] J. Bae, *et al.*, "Network-based rehabilitation system for improved mobility and tele-rehabilitation," *Control Systems Technology, IEEE Transactions on*, vol. 21, no. 5, pp. 1980–1987, 2013.
[19] A. Morbi, *et al.*, "Stability-guaranteed assist-as-needed controller for powered orthoses," *IEEE Transactions on Control Systems Technology*, vol. 22, no. 2, pp. 745–752, March 2014.
[20] J.-H. Ryu, *et al.*, "Stability guaranteed control: Time domain passivity approach," *IEEE Transactions on Control Systems Technology*, vol. 12, no. 6, pp. 860–868, 2004.
[21] J.-H. Ryu, *et al.*, "Time domain passivity control with reference energy following," *IEEE Transactions on Control Systems Technology*, vol. 13, no. 5, pp. 737–742, 2005.
[22] N. Chopra, *et al.*, "Bilateral teleoperation over unreliable communication networks," *IEEE Transactions on Control Systems Technology*, vol. 16, no. 2, pp. 304–313, 2008.
[23] M. Vidyasagar, *Nonlinear systems analysis*. SIAM, 2002, vol. 42.
[24] P. R. Culmer, *et al.*, "A control strategy for upper limb robotic rehabilitation with a dual robot system," *IEEE/ASME Transactions on Mechatronics*, vol. 15, no. 4, pp. 575–585, 2010.
[25] S. F. Atashzar, *et al.*, "Control of time-delayed telerobotic systems with flexible-link slave manipulators," in *IEEE/RSJ International Conference on Intelligent Robots and Systems*. IEEE, 2012.
[26] K. Hashtrudi-Zaad and S. E. Salcudean, "Analysis of control architectures for teleoperation systems with impedance/admittance master and slave manipulators," *The International Journal of Robotics Research*, vol. 20, no. 6, pp. 419–445, 2001.
[27] H. K. Khalil and J. Grizzle, *Nonlinear systems*. Prentice hall, Upper Saddle River, 2002, vol. 3.
[28] T. Tsuji, *et al.*, "Human hand impedance characteristics during maintained posture," *Biol. cybernetics*, vol. 72, pp. 475–485, 1995.
[29] L. Masia and V. Squeri, "A modular mechatronic device for arm stiffness estimation in human-robot interaction," *IEEE/ASME Transactions on Mechatronics*, vol. PP, no. 99, pp. 1–14, 2014.
[30] M. Dyck and M. Tavakoli, "Measuring the dynamic impedance of the human arm without a force sensor," in *IEEE Int. Conf. on Rehab. Robotics*, 2013.
[31] A. Karime, *et al.*, "Cahr: A contextually adaptive home-based rehabilitation framework," *Instrumentation and Measurement, IEEE Transactions on*, vol. 64, no. 2, pp. 427–438, Feb 2015.
[32] E. Nuno, *et al.*, "A globally stable pd controller for bilateral teleoperators," *IEEE Tran. on Robotics*, vol. 24, no. 3, pp. 753–758, 2008.
[33] A. Aziminejad, *et al.*, "Transparent time-delayed bilateral teleoperation using wave variables," *IEEE Transactions on Control Systems Technology*, vol. 16, no. 3, pp. 548–555, 2008.
[34] J. Forbes and C. Damaren, "Passive linear time-varying systems: State-space realizations, stability in feedback, and controller synthesis," in *American Control Conference*, June 2010, pp. 1097–1104.
[35] A. Jazayeri, *et al.*, "Stability analysis of teleoperation systems under strictly passive and non-passive operator," in *World Haptics Conference*, April 2013, pp. 695–700.
[36] D. J. Hill and P. J. Moylan, "Stability results for nonlinear feedback systems," *Automatica*, vol. 13, no. 4, pp. 377–382, 1977.
[37] B. Hannaford and J.-H. Ryu, "Time-domain passivity control of haptic interfaces," *IEEE Transactions on Robotics and Automation*, vol. 18, no. 1, pp. 1–10, 2002.
[38] Y. Ye, *et al.*, "A power-based time domain passivity control for haptic interfaces," *IEEE Transactions on Control Systems Technology*, vol. 19, no. 4, pp. 874–883, 2011.
[39] V. Chawda and M. OMalley, "Position synchronization in bilateral teleoperation under time-varying communication delays," *IEEE/ASME Transactions on Mechatronics*, vol. 20, no. 1, pp. 245–253, Feb 2015.

S. Farokh Atashzar (S'11) obtained his B.Sc. degree in Electrical Engineering/Control Systems from K. N. Toosi University of Technology, Tehran, Iran, in 2008 and his M.Sc. degree in Mechatronics from Amirkabir University of Technology, Tehran, Iran, in 2011. Farokh joined the Western University, Ontario, Canada, in 2011, to pursue his Ph.D. degree under the supervision of Dr. Rajni Patel. In 2011, he was a doctoral trainee in the NSERC CREATE program in Computer-Assisted Medical Intervention (CAMI). His research work is being carried out at Canadian Surgical Technologies and Advanced Robotics (CSTAR), London, Ontario, Canada. He was a visiting research scholar at the University of Alberta, Canada, in 2014. During his Ph.D., He has received several awards including the prestigious Ontario Graduate Scholarship (OGS) in 2013.

Mahya Shahbazi (S'10) received the B.Sc. degree in Electrical Engineering from K. N. Toosi University of Technology, Tehran, Iran, in 2008, and the M.Sc. degree in mechatronics from Amirkabir University of Technology, Tehran, in 2011. She is currently working toward the Ph.D. degree at Western University, Ontario, Canada under the supervision of Dr. Rajni Patel. She was a doctoral trainee in the NSERC CREATE program in Computer-Assisted Medical Interventions and is a research assistant at Canadian Surgical Technologies and Advanced Robotics (CSTAR). She was a visiting research scholar at the University of Alberta, Canada, and also among the very few international students at Western University granted the prestigious OGS (Ontario Graduate Scholarship) award in 2014.

Mahdi Tavakoli (M'08) is an Associate Professor in the Dept. of Electrical and Computer Engineering, University of Alberta, Canada. He received his B.Sc. and M.Sc. degrees in Electrical Engineering from Ferdowsi University and K.N. Toosi University, Iran, in 1996 and 1999, respectively. He received his PhD degree in Electrical and Computer Engineering from the Western University, London, Ontario, Canada, in 2005. In 2006, he was a post-doctoral researcher at Canadian Surgical Technologies and Advanced Robotics (CSTAR), Canada. In 2007-2008, he was an NSERC Post-Doctoral Fellow at Harvard University, USA. Dr. Tavakolis research interests broadly involve the areas of robotics and systems control. He is currently on the Editorial Board of the Journal of Medical Robotics Research.

Rajni V. Patel (M'76, SM'80, F'92, LF'13) received the PhD degree in Electrical Engineering from the University of Cambridge, England, in 1973 and currently holds the position of Distinguished University Professor and Tier-1 Canada Research Chair in the Dept. of Electrical and Computer Engineering with cross appointments in the Dept. of Surgery and the Dept. of Clinical Neurological Sciences at Western University, London, Ontario, Canada. He also serves as Director of Engineering for Canadian Surgical Technologies and Advanced Robotics (CSTAR), Canada. He has served on the editorial boards of the IEEE Transactions on Robotics, the IEEE/ASME Transactions on Mechatronics, the IEEE Transactions on Automatic Control, and Automatica, and is currently on the Editorial Board of the International Journal of Medical Robotics and Computer Assisted Surgery and the Journal of Medical Robotics Research.